

# Time-Resolved Fluorescence Studies of Ribonuclease T<sub>1</sub> in Reversed Micelles

Maurice R. Eftink,<sup>1</sup> Zanchi Chen,<sup>1</sup> and Zygmunt Wasylewski<sup>2</sup>

Received December 18, 1995; accepted July 29, 1996

Time-resolved fluorescence intensity and anisotropy decay data were obtained for ribonuclease T<sub>1</sub> entrapped in bis(2-ethylhexyl) sodium sulfosuccinate/heptane reverse micelles, as a function of the size of the inner water pool at neutral pH. Data have been presented previously to show that this protein retains its native structure and undergoes reversible thermal unfolding in these reverse micelles (Shastry and Eftink, *Biochemistry* **36**, in press). The fluorescence decay of entrapped protein is similar to that for the protein in buffer. The rotational correlation time of entrapped ribonuclease T<sub>1</sub> is found to be longer than that in buffer; this rotational correlation time decreases with increasing size of the water pool but is still over twice the value for the protein in buffer for the largest size of water pool investigated, indicating an increased microviscosity within the reverse micelle. Thermal unfolding of the protein results in a significant decrease in the rotational correlation time of the entrapped proteins, consistent with the protein being unfolded but not interacting with the inner surfactant wall of the reverse micelle.

**KEY WORDS:** Ribonuclease T<sub>1</sub>; fluorescence lifetimes; fluorescence anisotropy decay; reversed micelles.

## INTRODUCTION

The encapsulation of proteins into reversed micelles has produced surprising effects on the properties of these macromolecules. In some cases, enzymatic activity has been retained in these microemulsions, which are often comprised over 95% hydrocarbon solvent. The long-term stability of some proteins is greatly enhanced by encapsulation. Since there are practical applications of such entrapped enzymes, there has been interest in determining the factors that influence the structural and functional properties of the proteins.<sup>(1-3)</sup>

Reversed micelles are formed by the addition of certain surfactants, such as bis(2-ethylhexyl) sodium sulfosuccinate (AOT), plus aqueous solution to a major

phase of organic solvent, such as *n*-heptane or isooctane.<sup>(1)</sup> The surfactant forms an interface between the organic phase and the spherical water pools. The size of the water pool depends on the amount of water added; this can be described by the ratio of moles of water per moles of AOT,  $W_0$ . The entrapped water is thought to be more structured than bulk water.<sup>(2)</sup> Within certain ranges of water content and AOT concentration (e.g.,  $W_0$  from 5 to 50), the reversed micelles form pseudo-stable microemulsions. The radius of the water pool may be between 10 and 80 Å<sup>(1,4)</sup> (for the AOT system an approximate relationship between  $W_0$  and this inner radius,  $r$  (Å), is  $r \approx 1.75 \cdot W_0$ ).<sup>(2)</sup> Such pool radii are large enough to include small proteins, plus one or more layers of waters of hydration (for both the proteins and the negatively charged sulfate groups lining the AOT interface).

To understand the effect of such encapsulation on the structural and functional properties of proteins, we must rely on spectroscopic and thermodynamic ap-

<sup>1</sup> Department of Chemistry, University of Mississippi, University, Mississippi 38677.

<sup>2</sup> Department of Biochemistry, Jagiellonian University, Krakow, Poland.

proaches. An important, fundamental question is how the charged micellar interface or the entrapped water molecules influence the structure, dynamics, and stability of a protein. Do such influences depend on the net charge of the interface (and/or entrapped protein) or on the size of the water pool? Can an entrapped protein undergo a reversible unfolding transition, or does the micelle in some way (either physically or kinetically) limit (or potentiate) the unfolding process. Battistel and co-workers<sup>(5)</sup> used differential scanning calorimetry to study the thermal unfolding of ribonuclease A, lysozyme, and cytochrome *c* in AOT reversed micelles. They found that these three proteins were each destabilized, toward thermal unfolding, when entrapped, and in each case the unfolding process was found to be irreversible. We have found that ribonuclease T<sub>1</sub> undergoes reversible unfolding in AOT reverse micelles (both AOT and the protein being negatively charged at the experimental pH) and that the free energy of unfolding of the entrapped protein is similar to that for the protein in buffer at neutral pH.<sup>(6)</sup>

Related questions are whether the entrapped protein is free to rotate within the water pool, whether the entrapped protein interacts with the micellar interface, and the extent to which the water molecules have interfacial or bulk qualities. Insight into each of these questions would help in understanding the structural and functional properties and stability of the entrapped proteins.

Here we present time-resolved fluorescence studies with ribonuclease T<sub>1</sub> entrapped in AOT reversed micelles, as a function of the size of the water pools, to characterize the rotational motion of this protein and to complement our above-mentioned thermodynamic studies. The fluorescence of the single tryptophan residue, Trp-59, of ribonuclease T<sub>1</sub> has a characteristic blue-shifted emission and its fluorescence and anisotropy decays are both close to being monoexponential in solution at neutral pH.<sup>(7-10)</sup> For these reasons, ribonuclease T<sub>1</sub> serves as an excellent probe for studying interactions with the AOT micellar interface and effects of the size of the water pool in a reverse micelle on such interactions.

## MATERIALS AND METHODS

**Materials.** Ribonuclease T<sub>1</sub> was provided by Dr. C. N. Pace, Texas A&M University. Sodium bis(2-ethylhexyl) sulfosuccinate (AOT), *n*-heptane, and *n*-decane were obtained from Sigma Chemical Co. (St. Louis, MO). The protein was dissolved in 0.05 M PIPES buffer, pH 7.0.

The reversed micelles were prepared by first adding solid AOT to 2 ml of the alkane to achieve the desired concentration (i.e., 150 or 300 mM). This solution was shaken by hand until the AOT was completely dissolved. Then a 0.02-ml aliquot of protein (dissolved in the above buffer at a concentration of ~2 mg/ml) and a variable volume of buffer was added to achieve the desired  $W_0$  ratio ( $W_0 = [\text{H}_2\text{O}]/[\text{AOT}]$ ). This mixture was shaken until clear. The  $W_0$  ratios in this study form stable microemulsions.

Fluorescence intensity and anisotropy decay data were obtained with an ISS (ISS Inc, Champaign, IL) phase/modulation fluorometer, equipped with an Innova 200 argon ion laser.<sup>(11)</sup> The 300- to 305-nm lines of this laser were used for excitation. Emission was monitored using a Corning 7/60 bandpass filter. The exciting beam was modulated using a Pockels cell over the range of 10–160 MHz. *p*-Terphenyl was used as a fluorescence lifetime reference ( $\tau = 1.0$  ns). Glans-Thompson polarizers were used for the anisotropy decay measurements. Temperature was controlled using a water-jacketed cell holder and a refrigerated water bath.

Raw phase and modulation data were analyzed, using equations described elsewhere,<sup>(12)</sup> by describing the intensity decays as a sum of exponentials decay law (using ISS software)

$$I(t) = I_0 \sum \alpha_i \exp(-t/\tau_i) \quad (1)$$

where  $I(t)$  is the intensity as a function of time,  $t$ ,  $I_0$  is the intensity at  $t = 0$ ,  $\tau_i$  is the decay time for component  $i$ , and  $\alpha_i$  is the normalized amplitude associated with this component. The fractional intensity of component  $i$  is defined as  $f_i = \alpha_i \tau_i / \sum \alpha_i \tau_i$ . Likewise, anisotropy decay [ $r(t)$ ] data were analyzed in terms of a sum of exponentials law,

$$r(t) = r_0 \sum g_i \cdot \exp(-t/\phi_i) \quad (2)$$

where  $r_0$  is the anisotropy for a completely immobilized fluorophore, and  $\phi_i$  is the rotational correlation time having amplitude  $g_i$ . The nonlinear least-squares fits were performed using ISS software and the analysis was non-associated (with respect to the intensity decay times and rotational correlation times). For biexponential fits, the value of  $r_0$  was fixed at 0.32.

## RESULTS

Before presenting the results, let us recall that there are three components to the type of reverse micelles used in these studies. These components are the organic phase, the aqueous phase, and the detergent AOT. Most

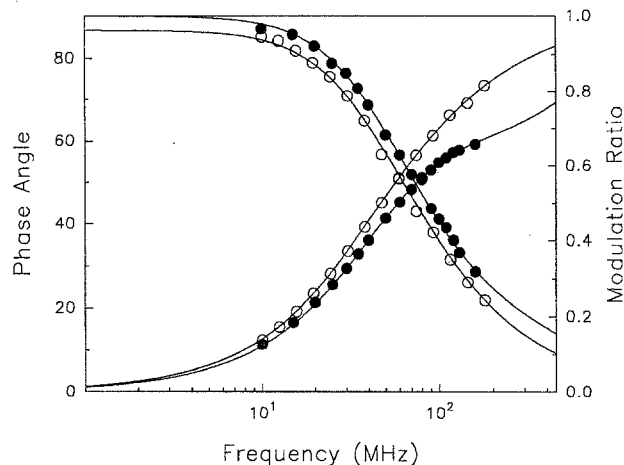


**Fig. 1.** Frequency-domain fluorescence lifetime data for ribonuclease T<sub>1</sub> in buffer (○) and in AOT:heptane reversed micelles at  $W_o = 10$  (●). Solid lines are fits to Eq. (1) with the following parameters: for buffer,  $\tau_1 = 3.85$  ns,  $\tau_2 = 1.51$  ns,  $f_1 = 0.895$ , and  $\chi^2 = 1.51$ ; for AOT reverse micelles at  $W_o = 10$ ,  $\tau_1 = 3.45$  ns,  $\tau_2 = 0.43$  ns,  $f_1 = 0.889$ , and  $\chi^2 = 1.48$ .

studies were done with *n*-heptane as organic solvent, while a few studies were done with *n*-decane to investigate the effect of increased viscosity of the organic phase. The concentration of AOT was either 150 or 300 mM. The water content, given in terms of the  $W_o$  ratio, was varied between 5 and 25 in this study. This range has previously been shown to form stable microemulsions.<sup>(4)</sup>

Elsewhere we have presented steady-state fluorescence and CD spectral data for ribonuclease T<sub>1</sub> entrapped in AOT reverse micelles at pH 7.<sup>(6)</sup> This protein retains its characteristic blue-shifted and structured fluorescence ( $\lambda_{\text{max}} = 325$  nm in buffer, which blue-shifts slightly to 322 nm in the AOT reverse micelles). Also, the aromatic and far-UV circular dichroism (CD) spectra of entrapped ribonuclease T<sub>1</sub> is essentially unchanged from that in bulk solution. These results suggest that the structure of this protein persists when it is entrapped in AOT reverse micelles. In addition, under certain conditions this protein was found to undergo reversible thermal unfolding with a thermal transition temperature, enthalpy change, and free energy change that are similar to the respective parameters for the protein in buffer.<sup>(6)</sup> The fact that both the AOT surfactant and the protein are negatively charged at pH 7 is thought to be a key to these observations about the retention of structure and reversible unfolding. When a protein and the surfactant interface have opposite charges, electrostatic interactions, together with apolar interactions at the water-hydrocarbon interface, can alter the structure of a protein

and/or can cause an unfolding transition to be irreversible. With the ribonuclease T<sub>1</sub>-AOT system, electrostatic interactions with the interface should be repulsive for both native and unfolded states. The consequence seems to be that the native structure of this protein is not perturbed by entrapment and that its thermal unfolding can be reversible.

*Time-Resolved Fluorescence Intensity Studies.* Fluorescence lifetime measurements were made at 20°C as a function of the [H<sub>2</sub>O]/[AOT] ratio,  $W_o$ , from 5 to 25 using heptane as the organic phase. Shown in Fig. 1 is an example of multifrequency phase modulation data for the protein in a reversed micelle ( $W_o = 10$ ) and in buffer. The data are very similar; in both cases the data can be described by a biexponential decay law, with a long  $\tau_1$  of  $\sim 4$  ns that dominates (fractional intensity of 85–93%) the decay. Actually the decay of the protein is nearly a monoexponential in buffer (89% of the intensity decaying with  $\tau_1 = 3.5$  ns, with  $\tau_2 = 0.43$  ns for the minor component). In the reversed micelles the 7–15% contribution from the short decay time ( $\tau_2$ , ranging from 0.4 to 1.2 ns) may be partially due to a contribution from light scattering. The decay profiles for entrapped ribonuclease T<sub>1</sub> do not change much from  $W_o = 5$  to 25. Shown in Fig. 2A is a plot of the long decay time,  $\tau_1$ , as a function of  $W_o$ . The value of  $\tau_1$  appears to increase slightly with increasing  $W_o$ . When decane is used as the organic phase, the fluorescence decay profiles are very similar to those using heptane (see open symbols in Fig. 2A). When the entrapped protein is subjected to a temperature of 60°C, which is sufficient to induce nearly complete thermal unfolding of the entrapped protein,<sup>(6)</sup> the intensity decay becomes faster and more heterogeneous ( $\tau_1 = 2.95$  ns,  $\tau_2 = 1.17$  ns,  $f_1 = 0.398$ ).

*Time-Resolved Fluorescence Anisotropy Decay Studies.* Figure 3 shows an example of anisotropy decay data for the protein in buffer and entrapped in AOT:heptane reverse micelles at a  $W_o$  of 15. In buffer, the anisotropy decay is well described by a monoexponential decay time of  $\phi = 5.8$  ns, a value that is consistent with previous reports[8–10]. In the  $W_o = 15$  reverse micelle, the anisotropy decay of the protein was fitted by a biexponential decay law with a dominate rotational correlation time,  $\phi_1$ , of 17.9 ns ( $r_{\infty}g_1 = 0.284$ ), with a small contribution from a subnanosecond component ( $\phi_2 = 0.34$  ns,  $r_{\infty}g_2 = 0.036$ ). Values of  $\phi_1$  and  $r_{\infty}g_1$  for other  $W_o$  values are given in Table I. A biexponential anisotropy decay law was usually required, but in a couple of cases the decay was essentially a monoexponential. For the biexponential cases, the contribution from the short rotational correlation time,  $\phi_2$ , is always less than 20% of the total  $r_{\infty}$  amplitude.

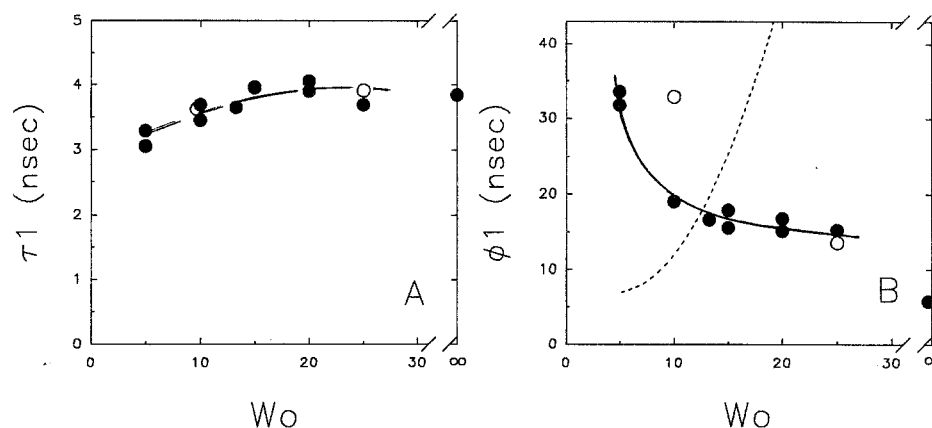


**Fig. 2.** (A) Dependence of the long fluorescence decay time,  $\tau_1$ , on  $W_0$  for ribonuclease T<sub>1</sub> entrapped in AOT reverse micelles, using heptane (●) or decane (○) as the organic phase. The entry at  $W_0 = \infty$  is the long  $\tau$  value for the protein in buffer. (B) Dependence of the long rotational correlation time,  $\phi_1$ , on  $W_0$  for entrapped ribonuclease T<sub>1</sub>, using heptane (●) or decane (○) as the organic phase. The dashed curve is the expected value of  $\phi_{mic}$  for global rotation of the AOT reverse micelle as a function of  $W_0$  (from Ref. 19). These  $\phi_{mic}$  are for AOT reverse micelles in isoctane at 25°C, which is a slightly different condition from that used here, but the ascending trend should still hold. The entry at  $W_0 = \infty$  is the  $\phi_1$  in buffer.

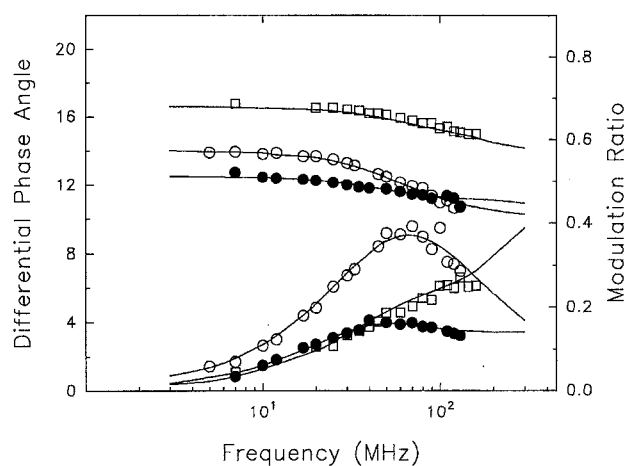


**Fig. 3.** Differential polarized phase-modulation anisotropy decay data for ribonuclease T<sub>1</sub> in buffer (○) at 20°C, in AOT:heptane,  $W_0 = 15$  reversed micelles (●) at 20°C, and in AOT:heptane,  $W_0 = 15$  reverse micelles (□) at 60°C. See Table I for fitting parameters.

The long  $\phi_1$  value appears to be related to global rotation of the protein and/or the protein–reverse micelle structure. As shown in Fig. 2B, the long  $\phi_1$  value is largest for  $W_0 = 5$  reversed micelles;  $\phi_1$  decreases with increasing  $W_0$ , but the limiting value at  $W_0 = 25$  is still about 2.5-fold larger than the value of  $\phi_1$  for the protein in buffer. Anisotropy decay data at 60°C show faster motion, with the long  $\phi_1$  reduced to 3.67 ns and with a significant contribution (i.e.,  $r_0 g_2 / \sum R_0 g_i = 66\%$ ) from a faster rotational correlation time,  $\phi_2 = 0.35$  ns.

**Table I.** Time-Resolved Fluorescence Intensity and Anisotropy Decay Parameters for Ribonuclease T<sub>1</sub> Entrapped in AOT Reverse Micelles<sup>a</sup>

$W_0$	$\phi_1$ (ns)	$r_0 g_1$	$\phi_2$ (ns)	$r_0 g_2$	$\chi^2$
5	33.6	0.223	0.31	0.097	3.0
5	31.8	0.269	0.24	0.05	1.2
10	19.1	0.271	0.03	0.049	0.8
13.3	16.7	0.301	—	—	0.64
15	15.6	0.305	—	—	1.2
15	17.9	0.284	0.34	0.036	0.30
20	16.8	0.259	0.27	0.061	0.60
20	15.2	0.297	0.82	0.023	2.40
25	15.3	0.248	2.04	0.072	2.4
15 (60°C) <sup>b</sup>	3.67	0.109	0.35	0.211	0.90
10 <sup>c</sup>	32.9	0.243	0.071	0.077	2.30
25 <sup>c</sup>	13.6	0.249	0.05	0.071	4.0
Buffer <sup>d</sup>	5.79	0.322	—	—	0.6

<sup>a</sup> Data at 20°C, unless noted, at pH 7, 0.05 M PIPES buffer with *n*-heptane as the organic phase. Excitation at 300 nm. Fits are to Eq. (2) with  $r_0$  fixed at 0.32, except for fits to a monoexponential decay law.  $\chi^2$  values calculated using standard deviations for the phase and modulation data of 0.4° and 0.01, respectively.

<sup>b</sup> Data at 60°C.

<sup>c</sup> Using *n*-decane as the organic phase.

<sup>d</sup> Protein in buffer.

Data were also collected for AOT reversed micelles formed in *n*-decane, a solvent having a higher viscosity than *n*-heptane (0.387 cP for heptane, 0.838 cP for decane at 25°C; *CRC Handbook of Chemistry and Physics*, 75th ed.). The  $\phi_1$  value for  $W_0 = 10$  micelles in decane

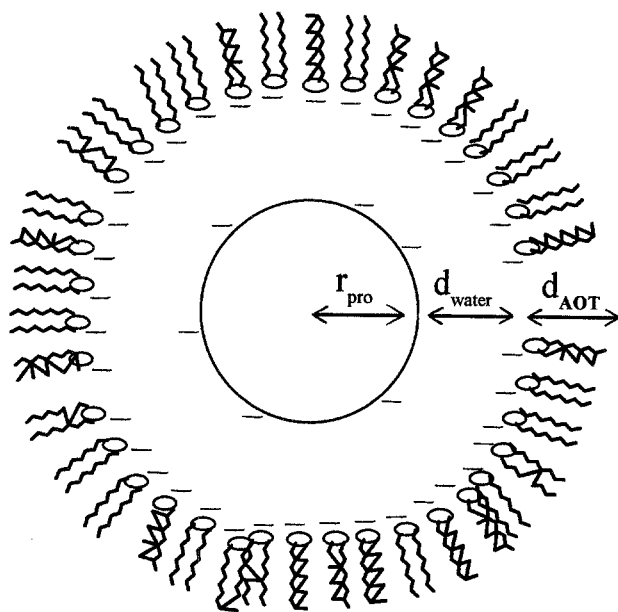


Fig. 4. Model for the protein entrapped in AOT reverse micelles. The distances  $r_{\text{pro}}$ ,  $d_{\text{water}}$ , and  $d_{\text{AOT}}$  are defined by the drawing. Both the protein and the AOT sulfosuccinate head groups are negatively charged. The inner water pool contains water and counter- and coions.

has a significantly larger value (33 ns) than the corresponding  $\phi_1$  value for  $W_o = 10$  micelles in heptane ( $\sim 20$  ns). With increasing  $W_o$ , the value of  $\phi_1$  using decane becomes similar in magnitude to that using the less viscous heptane.

## DISCUSSION

A number of time-resolved fluorescence studies have been performed with proteins entrapped in reverse micelles. The results of such studies seem to depend on the degree to which the protein interacts electrostatically with the charged inner wall of the micelle and on whether the protein undergoes an induced conformational change upon incorporation. In some cases, including myelin basic protein and the polypeptides adrenocorticotropin and glucagon, there is evidence from CD data for an induced change in  $\alpha$ -helix content upon entrapment and interaction with the micellar environment.<sup>(13,14)</sup> In other cases, the secondary structure of the entrapped protein does not appear to be changed.<sup>(15,16)</sup> It is commonly found that the rotational correlation time of the entrapped protein is longer than its value in buffer. In some cases this longer rotational correlation time is found to increase with increasing  $W_o$ ,<sup>(14,17)</sup> but the more frequent observation seems to be that the rotational cor-

relation time decreases with increasing  $W_o$ .<sup>(13-16,18)</sup> Since ribonuclease T<sub>1</sub> in AOT reverse micelles is, to our knowledge, the only case where reversible unfolding occurs (which we have argued is due to a repulsive interaction between the like-charged protein and the inner micelle wall) and since CD, steady-state fluorescence, and thermal unfolding data strongly suggest that entrapped ribonuclease T<sub>1</sub> retains its native structure,<sup>(6,23)</sup> we have investigated the effect of increasing  $W_o$  on its rotational freedom. Also, the fact that ribonuclease T<sub>1</sub> has a single internal tryptophan residue and that its fluorescence anisotropy decay in buffer is a monoexponential, and the intensity decay is nearly a monoexponential at pH 7, makes this a good protein for studies with reverse micelles.

The present time-resolved intensity and anisotropy decay studies support the interpretation that the protein exists in its solution-phase three-dimensional structure in AOT reversed micelles, at least for the range of  $W_o = 5-25$ . The fluorescence lifetime components are similar for free and entrapped protein; over the entire range of  $W_o$ , the fractional intensity associated with the long  $\tau_1$  is 85-93%, a value similar to that for the protein in buffer. The anisotropy decay parameters differ significantly from the buffer-phase values and reflect the environment of the entrapped protein. The anisotropy decay is essentially a monoexponential in some cases, but usually a subnanosecond rotational correlation time with a low amplitude is needed for an adequate fit.

At  $W_o = 5$  the  $\phi_1$  is over 30 ns, which is much larger than the value of  $\sim 6$  ns for global rotation of the protein in buffer. We think that this indicates that the rotational motion of the protein is controlled by rotation of the entire micelle structure at low  $W_o$ . As  $W_o$  increases, with a concomitant increase in the size of the water pool, the long  $\phi_1$  decreases monotonically to  $\sim 15$  ns. The overall rotational correlation time of the micelle structures,  $\phi_{\text{mic}}$ , must increase as  $W_o$  increases (see the dashed line in Fig. 2B, which represents values of  $\phi_{\text{mic}}$  from Vos and co-workers<sup>(19)</sup>). The fact that  $\phi_1$  decreases with  $W_o$  indicates that the protein is able to rotate independently within the growing reverse micelle. At  $W_o = 5$ ,  $\phi_1$  must be approximately equal to  $\phi_{\text{mic}}$ . At  $W_o = 25$ ,  $\phi_1$  reflects rotational motion within the water pool, which is limited by the local microviscosity. Figure 4 depicts a model for entrapped protein. Assuming that the value of  $\phi_1$  at  $W_o = 5$  is due entirely to overall rotation of the micelle (i.e., that the protein does not rotate independently when the water pool radius is small), then the value of  $\phi_1$  should be equal to  $\eta V/kT$ , where  $\eta$  is the effective viscosity and  $V$  is the volume of the spherical micelle having effective radius,  $r_{\text{mic}} = r_{\text{pro}} + d_{\text{water}}$

+  $d_{\text{AOT}}$ , where the latter are the radius of the protein, the distance due to the water molecules, and the distance due to the AOT interfacial molecules. From  $\phi_1 = 32$  ns for the  $W_o = 5$  complex, we calculate  $r_{\text{mic}} = 43$  Å. Assuming  $r_{\text{pro}} = 18$  Å (calculated from the molecular weight of the protein, 11.1 kDa, an assumed density of 1.3 g/ml, and assuming the protein to be spherical) and  $d_{\text{AOT}} = 12$  Å,<sup>(4,19)</sup> the distance due to the water molecules can be calculated to be approximately equal to 13 Å. This would correspond to about six or seven water molecule layers between the protein and AOT interface. Much, if not all, of this water layer will be hydration water for the charged (mostly negatively) and polar groups on the protein surface and the negatively charged sulfosuccinate groups of AOT.

The value of  $\phi_1$  at high  $W_o$  is still 2.5 times larger than that for global rotation in bulk water. The simplest interpretation of the latter result is that the microviscosity experienced by the entrapped protein is greater than that of normal bulk water.<sup>(2)</sup> Previous anisotropy decay studies with entrapped small fluorophores, such as auramine *O* and *N*-acetyl-L-tryptophanamide, have indicated an apparent internal microviscosity of approximately 20 cP for  $W_o = 25$ .<sup>(20–22)</sup> The above  $\phi_{1,\text{reverse micelle}}/\phi_{1,\text{buffer}}$  ratio for ribonuclease is consistent with an internal microviscosity of 2.5–3 cP in the AOT reverse micelles at  $W_o = 25$ . This viscosity value is lower than that estimated using smaller probes, but this can be attributed to differences in the degree to which the probes and protein interact with the interface.

The measurements using decane as the organic phase provide support for the above argument that  $\phi_1$  reflects rotation of the entire micelle at low  $W_o$  and reflects rotation of the protein within a micelle at larger  $W_o$ . For  $W_o = 10$  the  $\phi_1$  for decane is 1.5 times the corresponding value in heptane; at higher  $W_o$  the  $\phi_1$  values is approximately the same for both organic solvents. Since the viscosity of decane is ~2.2-fold larger than that of heptane, the difference in  $\phi_1$  at  $W_o = 10$  for the two solvents can be attributed primarily to the effect of the increased viscosity of the organic phase on the rotation of an entire micelle.

Finally, the anisotropy decay of entrapped ribonuclease at 60°C (for  $W_o = 15$ ), which is above the apparent unfolding temperature for the protein in the AOT reverse micelles,<sup>(6)</sup> shows that the rotation of the entrapped unfolded protein is characterized by a  $\phi_1$  of 3.7 ns. This indicates that the unfolded protein is not immobilized by a strong interaction with the AOT interface and supports our previous interpretation that neither the native nor the unfolded protein interacts favorably with the micellar interface. Such an interpretation helps ex-

plain our observation that ribonuclease  $T_1$  undergoes reversible thermal unfolding when entrapped in AOT reverse micelles.

## ACKNOWLEDGMENT

This research was supported by NSF Grant MCB 94-07167 to M.R.E.

## NOMENCLATURE

$\alpha_i$	Amplitude of component <i>i</i> associated with fluorescence decay $\tau_i$
$f_i$	Fractional intensity associated with fluorescence decay time $\tau_i$
$\phi$	Rotational correlation time
$g_i$	Amplitude of component <i>i</i> associated with anisotropy decay $\phi_i$
$\lambda_{\text{max}}$	Fluorescence emission maximum
$r_o$	Fundamental anisotropy of an immobilized fluorophore
$\tau_i$	Fluorescence lifetime of component <i>i</i>
$W_o$	Ratio of water molecules per detergent molecules in a reverse micelle

## REFERENCES

1. P. L. Luisi and J. Magid (1986) *CRC Crit. Rev. Biochem.* **20**, 409–474.
2. P. L. Luisi, M. Giomini, M. P. Pileni, and B. H. Robinson (1988) *Biochim. Biophys. Acta* **947**, 209–246.
3. R. M. D. Verhaeret, R. Hilhorst, A. J. V. G. Visser, and C. Veeger (1992) in A. Gomez-Puyou (Ed.), *Biomolecules in Organic Solvents*, CRC Press, Boca Raton, FL, pp. 132–162.
4. M. Zulauf and H.-F. Eicke (1979) *J. Phys. Chem.* **83**, 480–486.
5. E. Battistel, P. L. Luisi, and G. Rialdi (1988) *J. Phys. Chem.* **92**, 6680–6685.
6. M. C. R. Shastry and M. E. Eftink (1996) *Biochemistry* **36**, 4094–4101.
7. J. W. Longworth (1968) *Photochem. Photobiol.* **7**, 587–592.
8. D. R. James, D. R. Dremmer, R. P. Steer, and R. E. Verral (1985) *Biochemistry* **24**, 5517–5526.
9. L. X.-Q. Chen, J. W. Longworth, and G. R. Fleming, (1987) *Biophys. J.* **51**, 865–873.
10. I. Gryczynski, M. R. Eftink, and J. R. Lakowicz (1988) *Biochim. Biophys. Acta* **954**, 244–252.
11. M. R. Eftink and C. A. Ghiron (1987) *Biophys. J.* **52**, 467–473.
12. J. R. Lakowicz, E. Gratton, G. Laczko, H. Cherek, and M. Limkeman (1984) *Biophys. J.* **46**, 463–477.
13. C. Nicot, M. Vacher, M. Vincent, J. Gallay, and M. Waks (1985) *Biochemistry* **24**, 7024–7032.
14. J. Gallay, M. Vincent, C. Nicot, and M. Waks (1987) *Biochemistry* **26**, 5738–5747.
15. A. J. W. G. Visser, J. van Engelen, N. V. Visser, A. van Hoek, R. Hilhorst, and R. B. Freedman (1994) *Biochim. Biophys. Acta* **1204**, 225–234.

16. V. J. Lenz, M. Federwisch, H.-G. Gattner, D. Brandenburg, H. Hocker, U. Hassiepen, and A. Wollmer (1995) *Biochemistry* **34**, 6130–6141.
17. V. N. Dorovska-Taran, C. Veeger, and A. J. W. G. Visser (1993) *Eur. J. Biochem.* **211**, 47–55.
18. P. Marzola and E. Gratton (1991) *J. Phys. Chem.* **95**, 9488–9495.
19. K. Vos, C. Laane, S. R. Weijers, A. van Hoek, C. Veeger, and A. J. W. G. Visser (1987) *Eur. J. Biochem.* **169**, 259–268.
20. M. Hasegawa, T. Sugimura, K. Kuraishi, Y. Shindo, and A. Kitahara (1992) *Chem. Lett.* 1373–1376.
21. D. M. Davis, D. McLoskey, D. J. S. Birch, R. M. Swart, P. R. Bellert, and R. S. Kittlety (1994) *Proc. SPIE* **2137**, 331–342.
22. M. Wong, J. K. Thomas, and M. Gratzel (1976) *J. Am. Chem. Soc.* **98**, 2391–2397.
23. A. Guz and Z. Wasylewski (1994). *J. Protein Chem.* **13**, 393–399.